



OC5 Project Phase I: Validation of Hydrodynamic Loading on a Fixed Cylinder

Preprint

A. Robertson, F. Wendt, J. Jonkman, Wojciech Popko, Fabian Vorpahl, Carl Trygve Stansberg, Erin E. Bachynski, Ilmas Bayati, Friedemann Beyer, Jacobus B. de Vaal, Rob Harries, Atshushi Yamaguchi, Hyunkyung Shin, Byungcheol Kim, Tjeerd van der Zee, Pauline Bozonnet, Borja Aguilo, Roger Bergua, Jacob Qvist, Wang Qijun, Xiaohong Chen, Matthieu Guerinel, Ying Tu, Huang Yutong, Rongfu Li, and Ludovic Bouy

See first page of paper for authors' affiliations

To be presented at the International Offshore and Polar Engineering Conference (ISOPE 2015)

Kona, Hawaii

June 21–26, 2015

**NREL is a national laboratory of the U.S. Department of Energy
Office of Energy Efficiency & Renewable Energy
Operated by the Alliance for Sustainable Energy, LLC**

This report is available at no cost from the National Renewable Energy Laboratory (NREL) at www.nrel.gov/publications.

Conference Paper

NREL/CP-5000-63567

April 2015

Contract No. DE-AC36-08GO28308

NOTICE

The submitted manuscript has been offered by an employee of the Alliance for Sustainable Energy, LLC (Alliance), a contractor of the US Government under Contract No. DE-AC36-08GO28308. Accordingly, the US Government and Alliance retain a nonexclusive royalty-free license to publish or reproduce the published form of this contribution, or allow others to do so, for US Government purposes.

This report was prepared as an account of work sponsored by an agency of the United States government. Neither the United States government nor any agency thereof, nor any of their employees, makes any warranty, express or implied, or assumes any legal liability or responsibility for the accuracy, completeness, or usefulness of any information, apparatus, product, or process disclosed, or represents that its use would not infringe privately owned rights. Reference herein to any specific commercial product, process, or service by trade name, trademark, manufacturer, or otherwise does not necessarily constitute or imply its endorsement, recommendation, or favoring by the United States government or any agency thereof. The views and opinions of authors expressed herein do not necessarily state or reflect those of the United States government or any agency thereof.

This report is available at no cost from the National Renewable Energy Laboratory (NREL) at www.nrel.gov/publications.

Available electronically at SciTech Connect <http://www.osti.gov/scitech>

Available for a processing fee to U.S. Department of Energy and its contractors, in paper, from:

U.S. Department of Energy
Office of Scientific and Technical Information
P.O. Box 62
Oak Ridge, TN 37831-0062
OSTI <http://www.osti.gov>
Phone: 865.576.8401
Fax: 865.576.5728
Email: reports@osti.gov

Available for sale to the public, in paper, from:

U.S. Department of Commerce
National Technical Information Service
5301 Shawnee Road
Alexandria, VA 22312
NTIS <http://www.ntis.gov>
Phone: 800.553.6847 or 703.605.6000
Fax: 703.605.6900
Email: orders@ntis.gov

Cover Photos by Dennis Schroeder: (left to right) NREL 26173, NREL 18302, NREL 19758, NREL 29642, NREL 19795.

NREL prints on paper that contains recycled content.

OC5 Project Phase I: Validation of Hydrodynamic Loading on a Fixed Cylinder

Amy N. Robertson¹, Fabian F. Wendt¹, Jason M. Jonkman¹, Wojciech Popko², Fabian Vorpahl^{2,3}, Carl Trygve Stansberg⁴, Erin E. Bachynski⁴, Ilmas Bayati⁵, Friedemann Beyer⁶, Jacobus B. de Vaal⁷, Rob Harries⁸, Atshushi Yamaguchi⁹, Hyunkyong Shin¹⁰, Byungcheol Kim¹⁰, Tjeerd van der Zee¹¹, Pauline Bozonnet¹², Borja Aguilo¹³, Roger Bergua¹³, Jacob Qvist¹⁴, Wang Qijun¹⁵, Xiaohong Chen¹⁶, Matthieu Guerinel¹⁷, Ying Tu¹⁸, Huang Yutong¹⁹, Rongfu Li²⁰, Ludovic Bouy²¹

1. National Renewable Energy Laboratory, Colorado, USA; 2. Fraunhofer IWES, Germany; 3. Vorpahl Wind Engineering Consultants, Germany; 4. MARINTEK, Norway; 5. Politecnico di Milano, Italy; 6. Stuttgart Wind Energy, University of Stuttgart, Germany; 7. Institute for Energy Technology, Norway; 8. DNV GL, England; 9. University of Tokyo, Japan; 10. University of Ulsan, Korea; 11. Knowledge Centre WMC, the Netherlands; 12. IFP Energies nouvelles, France; 13. Alstom Wind, Spain; 14. 4Subsea, Norway; 15. Dongfang Turbine Co., China; 16. ABS, USA; 17. WavEC Offshore Renewables, Portugal; 18. Norwegian University of Science and Technology, Norway; 19. Chinese General Certification, China; 20. Goldwind, China; 21. PRINCIPIA, France

ABSTRACT

This paper describes work performed during the first half of Phase I of the Offshore Code Comparison Collaboration Continuation, with Correlation project (OC5). OC5 is a project run under the International Energy Agency Wind Research Task 30, and is focused on validating the tools used for modeling offshore wind systems. In this first phase, simulated responses from a variety of offshore wind modeling tools were validated against tank test data of a fixed, suspended cylinder (without a wind turbine) that was tested under regular and irregular wave conditions at MARINTEK. The results from this phase include an examination of different approaches one can use for defining and calibrating hydrodynamic coefficients for a model, and the importance of higher-order wave models in accurately modeling the hydrodynamic loads on offshore substructures.

KEY WORDS: Offshore wind; code comparison; wave harmonics

INTRODUCTION

Offshore wind turbines (OWTs) are designed and analyzed using comprehensive simulation tools (or codes) that account for the coupled dynamics of the wind inflow, aerodynamics, elasticity, and controls of the turbine, along with the incident waves, sea current, hydrodynamics, mooring dynamics, and foundation dynamics of the support structure. The OC3 and OC4 projects (Offshore Code Comparison Collaboration and Offshore Code Comparison Collaboration Continuation), which operated under International Energy Agency (IEA) Wind Tasks 23 and 30, were created to verify the accuracy of OWT modeling tools through code-to-code comparisons. These projects were successful in showing the influence of different modeling approaches on the simulated response of offshore wind systems. Code-to-code comparisons, though, can only identify differences. They do not determine which solution is the most accurate. To address this limitation, an extension of Task 30 was initiated, which is called OC5. This project's objective is validating

offshore wind modeling tools through the comparison of simulated responses to physical response data from actual measurements. The project will examine three structures using data from both floating and fixed-bottom systems, and from both scaled tank testing and full-scale, open-ocean testing.

The first phase of OC5 is focused on examining the hydrodynamic loads on fixed cylinders. No wind turbine is present in these tests because the purpose is to examine hydrodynamic loads only, before moving on to the complexity of coupled wind/wave loads and dynamic system response. Because this is the first time the group has used measured test data, a simple structure is chosen to ease into the complications involved when using real data. The first phase was also used to develop the model calibration and validation processes that will be used by the group throughout the project. Two different sets of data will be examined in this phase, and this paper focuses on the validation work for the first data set, which came from MARINTEK.

MODEL AND TEST DESCRIPTION

The first test data examined in Phase I of OC5 were generated in the towing tank at MARINTEK in Trondheim, Norway, during two separate test campaigns (see references to Tests I and II in Marthinsen, 1996; Stansberg, 1995; and Stansberg, 1997 for more information). The tank is 80-m long, 10.5-m wide, and 10-m deep, and is equipped with a hydraulic double-flap longcrested wavemaker at one end. At the opposite end of the tank is a wave-absorbing beach, and the side walls contain wave absorbers. The test specimens were placed 38.6 m from the wave maker, in the middle of the tank width-wise.

The units tested were single steel cylinders with varying diameters. The draft of each was 1.44 m, meaning that the bottom surface of the cylinder is exposed to the water and the upper surface pierces the still water line (SWL). The cylinders were attached to a stiff framework through two force transducers at the SWL and at 0.7 m below (see Fig.

1). Vertical and transverse motions were restricted by stiffener rods between the framework and the cylinder. The force transducers recorded load along the wave propagation direction, with a stiff enough frame to warrant modeling the cylinder as fixed and rigid (the eigenfrequencies of the framework are 10 Hz and greater).

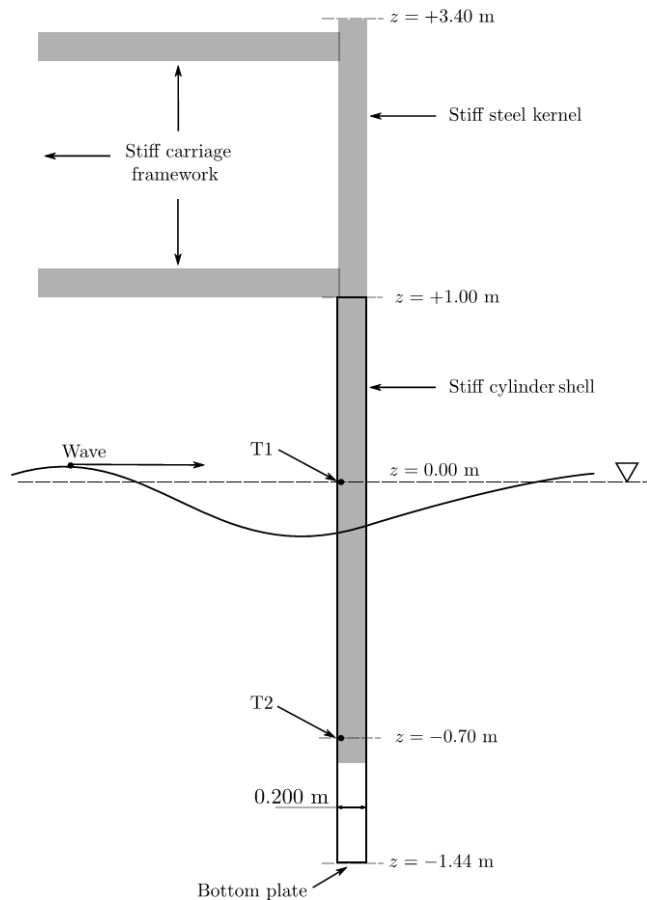


Fig. 1: Cylinder test configuration (Stansberg, 1997)

The instrumentation for the tests consisted of two strain gauge force transducers (T1 and T2 in Fig. 1), and three conductance-type wave probes. The data were recorded at 50-Hz sampling frequency and then real-time low-pass filtered at 20 Hz. The data were then filtered digitally using a low-pass filter (with no phase distortion) at 7.5 Hz to eliminate any of the framework structural response. The measurements that were used in this project include the undisturbed wave elevation measurement at the structure location (measured without the structure present), and the hydrodynamic surge force and pitch moment calculated from the two force transducer measurements.

The data to be used in this project are from two test campaigns using two different cylinders with diameters of 0.2 m and 0.327 m. For each of the cylinder sizes, a variety of regular and irregular wave tests were conducted. The same waves were used for the different cylinders in the test campaigns, allowing for the analysis of the influence of aspect ratio (length/diameter) on hydrodynamic loading (aspect ratios = 4.4 and 7.2). The irregular wave tests were run for 1710 s, while the regular wave tests were run for 120 s. The data were recorded with a 0.02-s timestep. A full list of the tests performed can be found in (Stansberg, 1997). From these available data sets, 20 were chosen for examination in this project (see Table 1). Sixteen regular and four irregular wave tests were considered. Based on the depth of the water, the waves can be considered deep-water waves.

Table 1: Data sets simulated in OC5 project, Phase I

OC5 Test No.	Original Test No.	Wave Type	Diameter (m)	H/Hs (m)	T/Tp (s)	γ
1	441	Regular	0.2	0.15	1.533	
2	444	Regular	0.2	0.23	1.533	
3	442	Regular	0.2	0.28	1.533	
4	445	Regular	0.2	0.37	1.533	
5	341	Regular	0.327	0.15	1.533	
6	344	Regular	0.327	0.23	1.533	
7	342	Regular	0.327	0.28	1.533	
8	345	Regular	0.327	0.37	1.533	
9	431	Regular	0.2	0.282	2.114	
10	433	Regular	0.2	0.45	2.114	
11	432	Regular	0.2	0.522	2.114	
12	434	Regular	0.2	0.6	2.114	
13	1331	Regular	0.327	0.282	2.114	
14	333	Regular	0.327	0.450	2.114	
15	332	Regular	0.327	0.522	2.114	
16	334	Regular	0.327	0.6	2.114	
17	401	Irregular	0.2	0.279	2.4	1.7
18	4301	Irregular	0.327	0.279	2.4	1.7
19	402	Irregular	0.2	0.357	2.76	1.7
20	4302	Irregular	0.327	0.357	2.76	1.7

T = wave period, Tp = peak wave period, γ = JONSWAP peak factor
H = wave height, Hs = significant wave height

MODELING APPROACH

The purpose of the work presented in this paper is to determine the ability of offshore wind modeling tools to accurately predict the hydrodynamic loads on fixed cylinders. A list of the tools used in this study is summarized in Table 2, which also shows the participant using the tool, and the modeling approach employed. Many of these tools are fairly new, but are based on well-established methods for modeling hydrodynamic loads. Other tools are ones that have been used extensively in the offshore industry, but have been modified or coupled to other software packages to enable the modeling of the aerodynamic turbine loads. The purpose here is to understand the different capabilities of these tools and how modeling choices affect the accuracy of their calculated hydrodynamic loads before moving on to systems with more complex geometry and coupling with turbine aerodynamic loads and control.

The experiment examined here is fairly simple in that there is no wind turbine present, the structure has a simple cylindrical geometry with no shadowing effects, the structure is fixed, and it is considered rigid. This allows us to focus on the influence of the wave theory and hydrodynamic load model on the calculated reaction loads. Results from Phase II of the OC4 project (see Robertson et al., 2014) showed significant discrepancies in the predicted response characteristics of the simulated semisubmersible wind turbine system between modeling tools, but the complexity of the system prevented a more in-depth analysis of the influence of the individual modeling approaches. This work will focus more directly on examining the applicability of different hydrodynamic modeling approaches.

Table 2: Summary of offshore wind modeling tools and modeling approach

Participant	Code	Wave Model	Hydro Model	Wave Surface
4SUBSEA	OrcaFlex	3 rd Order Dean SF	ME	IW
ABS	CHARM3D+FAST	Linear Airy	ME	IWV
ALSTOM	Samcef Wind Turbines	5 th Order Stokes/L.Airy	ME	IW/IWW
CGC	Bladed 4.3	Linear Airy	ME	IWW
DEC	Morison's Eq.	Linear Airy	ME	IWW
DNV GL	Bladed 4.6	6 th and 8 th Order SF/L. Airy	ME	IW/IWW
DNV GL	Bladed 4.6	Linear Airy	1 st Order PF	No
Goldwind	FAST	2 nd Order Stokes	PF	No
IFE	3DFLOAT	6 th Order SF/L. Airy	ME	IW/IWE
IFPEN/PRI	DeeplinesTM Wind	3 rd Ord. SF (actual)/L.Airy	ME	IW
MARINTEK	RIFLEX	2 nd Order Stokes (actual)	ME	IW
NREL	FAST	2 nd Order Stokes/Actual	ME	No
NREL	FAST	2 nd Order	2 nd Order PF	No
NTNU	Morison's Eq.	Linear Airy	ME	No
PoliMi	ILMAS	Linear Airy	ME	No
SWE	SIMPACK+HydroDyn	Linear Airy	ME	No
UTOKYO	CaSt	Linear Airy	ME	No
UOU	UOU + FAST	2 nd Order Stokes	ME	No
WAVEC	Wavec2Wire	2 nd Order Stokes/Actual	2 nd /1st Order PF	IWW
WMC	FOCUS6 (PHATAS)	3 rd Order SF/L. Airy	ME	IW/IWW

SF = Stream Function, ME = Morison's Equation, PF = Potential Flow, IW = Instantaneous Water level, IWW = Instantaneous Water level: Wheeler, IWE = Instantaneous Water Level: Extrapolation, IWV = Instantaneous Water Level: Vertical Stretching

Because of the simplicity of the problem, most of the participants chose to use a modeling approach consisting purely of Morison's equation (see Morison et al., 1950). For a fixed cylinder, Morison's equation is written as:

$$F = \frac{1}{2} C_D \rho D u |u| + C_M \rho \frac{\pi D^2}{4} \ddot{u} \quad (1)$$

where u is the x -velocity of the fluid, \ddot{u} is the acceleration, D is the cylinder diameter, ρ is the fluid density, C_D is the drag coefficient, C_M is the inertia coefficient, and F is the force per unit length on the cylinder. Morison's equation has been used extensively throughout the offshore wind community for calculating hydrodynamic loads (see e.g., Gudmestad and Moe, 1996; Sarpkaya and Isaacson, 1981), and the purpose of this study is to understand how the different capabilities available in offshore wind modeling tools will affect the resulting force calculation and how to best choose the parameters in the equation. Differences between the participants' modeling capabilities are related to the utilized wave model and the application of additional hydrodynamic load effects, such as wave stretching, to calculate the force up to the instantaneous water level. In addition, three participants

used a potential-flow approach (DNV GL, NREL, and WAVEC). In future work, the group would also like to include computational fluid dynamics (CFD) computations, but no participant was able to complete these during the first phase of the project.

The wave theories employed by participants consisted of linear Airy waves and higher-order models such as 2nd and 5th order Stokes theory, 3rd order Dean waves, and 3rd, 6th, and 8th order stream functions. In Table 2, those participants that have two wave models specified used the first one for the regular wave cases and the second for the irregular wave cases. In addition, some tools have the ability to directly input and use the measured wave elevation time histories from the experiments. NREL, MARINTEK, DNV GL, IFE, and IFPEN/PRI are the participants that used this approach for the irregular wave cases. Only the wave elevation is measured in the experiments, so a wave model is still needed to determine the distributed wave particle velocities and accelerations along the length of the cylinder. Wave stretching was considered by several project participants when using linear Airy waves.

CALIBRATION AND VALIDATION PROCEDURE

A major aspect of this phase was the development of calibration and validation methods for offshore wind turbine modeling tools that will be applied throughout the remainder of the OC5 project. Validation of the modeling tools will be achieved through the simulation of several different technologies spanning the design space for offshore wind systems across a variety of metocean conditions. In the end, one will only be able to say that the tools have been validated for the types of systems and conditions that have been examined. This phase examines one of many different model configurations that will need to be considered in the validation process.

The first step in this process was to develop a document describing the properties of the system to be modeled. Participants then developed a model of the structure based on the specification document within their modeling tool of choice. Consistent model properties among the project participants are vital to ensure that differences in the results originate from the utilized modeling approaches and not from differences in the model definition.

The next step was to calibrate the models, which is necessary when there are uncertainties in the model parameters. For this set of experiments, the geometry of the system was well known, but there were some uncertainties related to the wave characteristics and the appropriate parameter values to use to model the resulting hydrodynamic forces. For the waves, a height and period were specified, but it was found that these values were not exactly produced by the wavemaker, and that the appropriate values could change based on the theory used to model the wave. For the wave forces, most modeled the system using Morison's equation, which is defined using added mass ($C_A = C_M - 1$) and drag coefficients (C_D). The group examined the best methods for choosing the appropriate values to use for these coefficients. Calibration was performed with a subset of the available data sets (cases 2, 7, 10, and 15, demarcated through a beige coloring in Table 1). The wave and force measurements were provided for these cases so that participants had the opportunity to tune relevant parameters to achieve the best fit of the resulting load measurements. The goal was to accurately model the total hydrodynamic force on the cylinder.

After calibration was accomplished, the remaining data sets were used to validate the models. Of the remaining 16 data sets, only the wave time histories were supplied. Therefore, participants had the opportunity to calibrate the wave characteristics for each case based on

the provided time histories. The load time histories were not provided, so participants chose the hydrodynamic coefficients for these cases based either on the calibrated values from the calibration cases or based on published empirical/semi-empirical relationships (look-up tables). Participants then simulated these cases and validation was achieved through comparison of the simulated total hydrodynamic force to the experimental measurement. To examine more closely the influence of the wave theory, a subset of the cases were run with all participants using the same wave and hydrodynamic parameters (wave height, wave period, C_A , and C_D). The next section will review the results of both the calibration and validation steps.

RESULTS

Calibration

To prescribe a wave within an offshore wind modeling tool, one has the option of inputting directly a wave elevation time history (available in some tools), or using a wave modeling theory such as linear Airy waves, or higher-order theories such as a Stokes or stream function wave. Wave models require prescription of a wave height (or significant wave height for irregular waves) and period (or peak period for irregular waves). As part of the calibration work in this project, participants tuned the wave height and period for each of the four calibration test cases (2, 7, 10, and 15).

Four different methods were used to tune the value for the wave height. These methods include manual tuning by eyeballing the height of the wave, using the height of the dominant frequency peak of a Fourier transform of the wave, and averaging the differences between identified peaks and troughs in the data. The fourth method is a linear least-squares approach that tunes the wave height by finding the value that produces the least error when comparing the derived wave time history to the measured one. The least-squares method will result in different values of wave height based on the wave theory used, but the other three approaches should not. Table 3 summarizes the calibration method used by each of the participants. Tuning of the wave period used similar methods.

The results of the calibration are shown in Fig. 2 and Fig. 3. The wave height results are very similar between participants with the differences increasing as the wave height increases. The figure is grouped by method used for the calibration, and one can see some distinct correlation between the method used and the value found. Averaging of the peaks and troughs seems to be the most consistent between participants, and the least-squares approach seems to produce some of the lowest results. On the other hand, the results of the period calibration were very consistent between the methods used, and so it was decided that all participants would use the same wave period values.

The second set of calibration work that was performed was the tuning of hydrodynamic coefficients. The majority of the participants used a modeling approach employing only Morison’s equation, which is a strip-theory approach. The primary inputs for this model are the added mass coefficient, C_A , and the drag coefficient, C_D . The typical approach for choosing these values is to use a semi-empirical relationship (look-up table), in which the coefficients are chosen based on the Reynold’s (Re) and/or Keulegan-Carpenter (KC) number of the flow regime. The availability of reported hydrodynamic coefficients, however, for low Re and KC values as used in this experiment is limited. (The KC values for the data sets range from 0.10 to 10 and the Re values from 5×10^3 to 3×10^5 .) In addition, most of the reported values in literature consider an infinite cylinder that is completely submerged. For the examined experiments the cylinder pierces the surface and a free end is present in the water, so these values might not be appropriate. Therefore, some

participants chose a different methodology for tuning their hydrodynamic coefficients. In addition, the majority of participants used the same coefficients along the length of the cylinder, with the exception of Alstom, who varied this value along the length.

Table 3: Wave height and period calibration methods used by the participants

Participant	Wave Height Calibration Approach	Period Calibration Approach
4SUBSEA	Manual tuning	Frequency peak
ABS	Averaging peaks/troughs	Averaging zero-crossings
ALSTOM	Averaging peaks/troughs	Averaging zero-crossings
CGC	Averaging peaks/troughs	Frequency peak
DEC	Linear least squares	N/A
DNV GL	Averaging peaks/troughs	Averaging peaks/troughs
IFE	Averaging peaks/troughs	Averaging peaks/troughs
IFPEN/PRI	Averaging peaks/troughs	Averaging peaks/troughs
Goldwind	Averaging peaks/troughs	Averaging zero-crossings
MARINTEK	Actual time series, filtered	Actual time series
NREL	Linear least squares	Linear least squares
PoliMi	Frequency peak	Frequency peak
SWE	Frequency peak	Averaging zero-crossings
UTOKYO	Linear least squares	Manual tuning
UOU	Frequency peak	Frequency peak
WAVEC	Frequency peak	Frequency peak
WMC	Manual tuning	Manual tuning

Table 4: Calibration methods used for choosing C_A and C_D

Participant	C_D Calibration Method	C_A Calibration Method
4SUBSEA	1.0	Manual
ABS	1.0	Least squares
ALSTOM	Weighted least squares	Weighted least squares
CGC	Least squares	Least squares
DEC	Least squares	Least squares
DNV GL	0.0	Least squares
IFE	1.0	Match amplitudes
IFPEN/PRI	DNV	DNV
MARINTEK	Least squares	Least squares
NREL	1.0	Least squares
NTNU	1.0	Least squares
PoliMi	DNV	KC-based
SWE	Least squares	Least squares
UTOKYO	Least squares	Least squares
UOU	1.0	Morison method
WAVEC	Morison method	Morison method
WMC	1.0	KC-based

The methods used are summarized in Table 4. They include look-up table approaches (DNV and KC -based), a least-squares approach, and Morison’s method. In addition, some participants felt that varying the drag coefficient did not have a significant influence on the model because the flow regime was dominated by inertia, and therefore chose to set C_D to a value of 1.0 for all cases. For these four cases, the maximum of the added mass term in Morison’s equation was 10 to 20 times larger than the drag term; and, a change in the drag coefficient from 0.5 to 1 resulted in a negligible change in the maximum total force.

Those participants who used the DNV method used a look-up table from the DNV-RP-C205 standard (2010), which provides values based on a combination of KC number and smoothness. For the least-squares approach, Morison’s equation is treated as a computational approximation of the measured force, and the unknown coefficients, C_A and C_D , are varied until the difference between the calculated and measured force is minimized. Participants found improved results when modifying this approach to weight selected points (Weighted Least Square) in the minimization problem, such as the peaks and troughs, and when considering only a subset of the data in order to minimize the influence of potential phase mismatch in the calibration.

Morison’s method is based on the formulation of Morison’s equation. This approach examines specific points in the experimental data when the wave elevation is at a maximum or at zero. At maximum wave elevation, the x -velocity of the wave particles is also at a maximum and the x -acceleration is zero. In examining Morison’s equation (Eq. 1) for a fixed cylinder, we see that when the acceleration is at zero, the force per unit length on the cylinder is purely from the drag force (the first term on the right-hand side). By examining points in the data where the acceleration is zero, the measured horizontal force can be used to calculate C_D from the known values of u , D , and ρ . Using this approach, one can also calculate C_M by looking at points in the data where the wave height is zero, and thus u is also zero. Then, the second term on the right side in Eq. 1 can be used to derive C_M , and consequently C_A . Participants, however, found that this approach was problematic and gave inconsistent results.

The results of the hydrodynamic coefficient calibration are shown in Fig. 4 and Fig. 5. The values for C_D are varied, with the exception of those that chose to set it to a constant value. There is little consistency between the results for those using a least-squares approach, which points to the fact that the choice of drag coefficient had very little effect on the resulting hydrodynamic loads. C_A , on the other hand, showed more similarity between participants, but little consistency within the method used for calibration. The variations could be due to different interpretations of look-up tables, use of different sets of data for the Morison calculation, and the influence of wave theory on the least-squares method. The decision at the end of the calibration process was to move forward with validation work allowing participants to use their own calibrated values for the hydrodynamic coefficients and wave parameters; however, the general consensus was that either using look-up tables or weighted least-squares were the preferred approaches. In industrial design applications C_A and C_D are usually determined through experiments or lookup tables.

Validation

After the calibration was complete, participants simulated the remaining 16 data sets chosen for analysis. For these cases, the wave time history was supplied, so participants were able to calibrate the appropriate wave height for their simulations. Set wave periods of 1.533 and 2.114 s were used by all participants due to the insensitivity

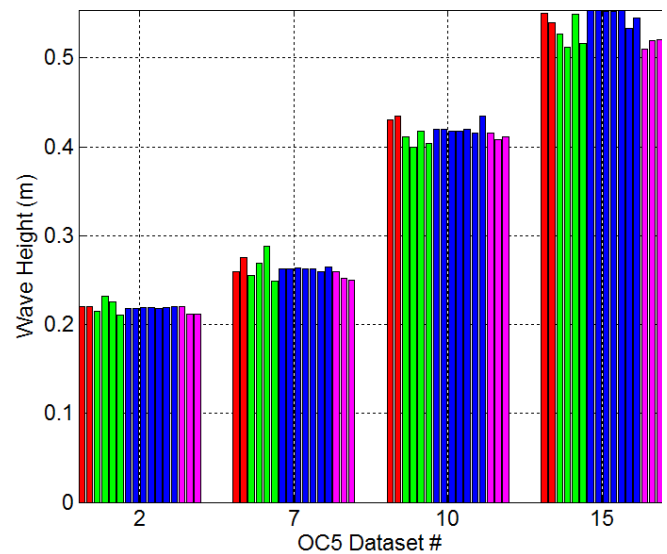


Fig. 2: Wave height calibration results: red = manual tuning; green = frequency peak; blue = average peaks/troughs; magenta = least squares

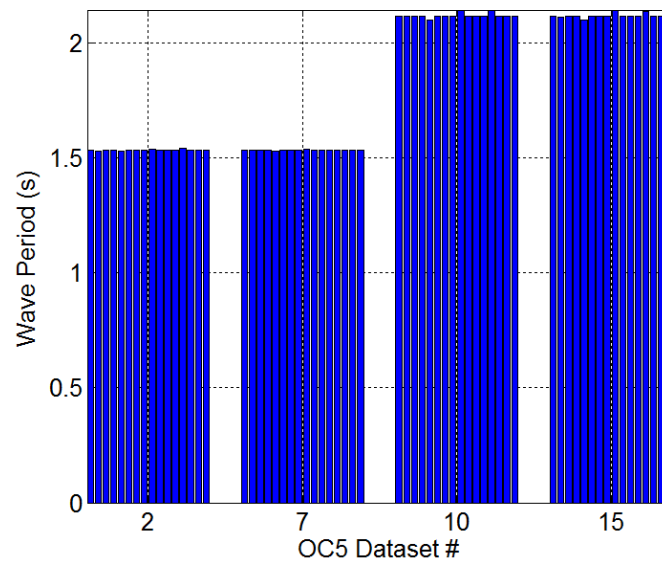


Fig. 3: Wave period calibration results; participants and approaches not delineated because of the consistency in the results

of period found in the calibration step. The hydrodynamic load data was not supplied, so participants had to decide how to choose the hydrodynamic coefficients for these cases—either based on the calibration work from the four initial cases or some other method.

The methods used by the participants for determining the remaining hydrodynamic coefficients are summarized in Table 5. Many of the approaches used for the calibration were used again, namely the use of look-up tables based either on Re or KC numbers. In addition, some modified the values from these look-up tables based on the findings from the calibration step. For instance, SWE used a least-squares fit to calibrate the hydrodynamic coefficients for the four calibration cases. For the validation, SWE used a look-up table, but modified the values based on the differences that their calibrated values had compared to these tables. The validation cases all consider experiments with the same diameter cylinder and same wave period as the calibration cases.

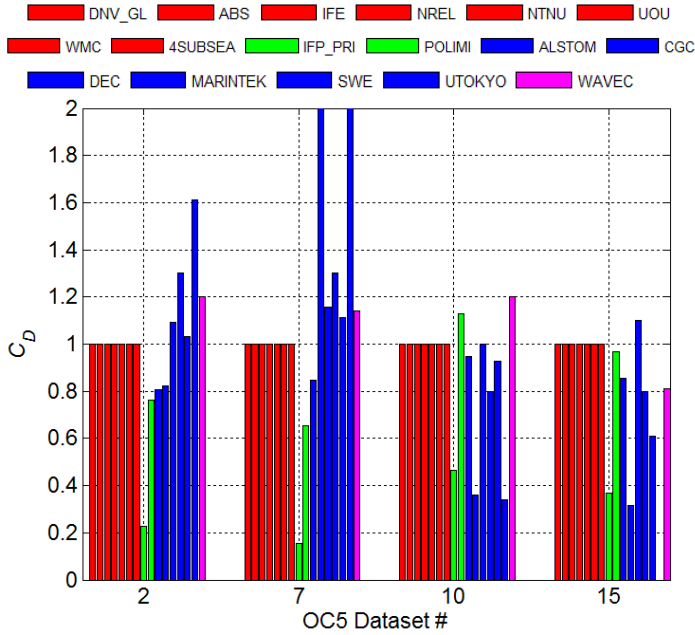


Fig. 4: C_D calibration results: red = set value; green = DNV; blue = least squares; magenta = Morison method

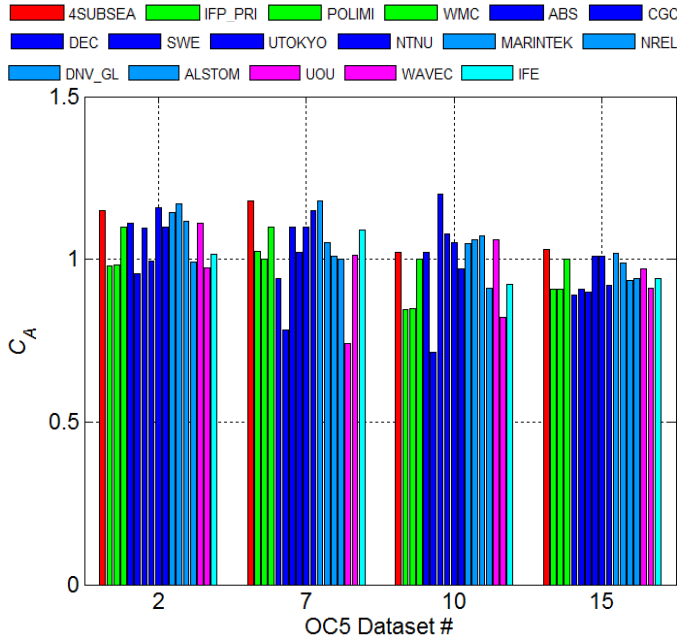


Fig. 5: C_A calibration results: red = manual; green = DNV/KC; dark blue = least squares (linear wave theory); light blue = least squares (higher-order wave theory); magenta = Morison method; cyan = match amplitudes

The only difference is the wave height of the cases. So, some participants used the calibrated values for cases that had the same diameter and period (D and T/Tp -based). IFE also considered the diffraction parameter (DP), which is the ratio of the diameter to wavelength, for choosing the value. MARINTEK used the MacCamy-Fuchs (MF) method for choosing the hydrodynamic coefficients for the irregular cases, modified based on the calibration.

Table 5: Methods Used for Choosing Hydrodynamic Coefficients for Validation Cases

Participant	C_D Method	C_A Method
4SUBSEA	1.0	KC -based
ABS	1.0	Re and KC -based
ALSTOM	DNV	DNV
CGC	Re - and KC -based	Re - and KC -based
DEC	Re -based	Re -based
DNV GL	0.0	Re -based
IFE	1.0	Re -, KC -, and DP -based
IFPEN/PRI	DNV	DNV
MARINTEK	D - and Tp -based, MF	D - and T/Tp -based, MF
NREL	1.0	D - and T/Tp -based
NTNU	1.0	D - and T/Tp -based
PoliMi	DNV	Manual
SWE	DNV with correction	DNV with correction
UOU	KC -based	KC -based with correction
WAVEC	DNV	KC -based
WMC	1.0	KC -based

The consistency between participants for the chosen hydrodynamic coefficients for the validation cases was similar to the consistency shown for the calibration cases, and so the results are not shown here.

Regular Wave Tests

Using the derived hydrodynamic coefficients, the participants simulated 12 regular wave cases. The wave conditions considered during these experiments are fairly benign. No breaking waves were present, but there was some level of nonlinearity, especially as wave height and steepness increased (as would be expected). Fig. 6 shows an example of the wave elevation time series, and resulting integrated hydrodynamic force in the x -direction along the cylinder for Test 4, which considers a 0.2-m diameter cylinder in regular waves with a height of 0.37 m and period of 1.533 s. The nonlinearity of the wave is evident in the wave elevation signal. Those models using linear wave theory are shown in red in the figure, and one can see that, in comparison, the experimental wave and higher-order wave models have narrower, increased peaks, and flatter, shallower troughs (as expected). The force results also show a shift in the peak for the experiment and higher-order wave models compared to those using linear waves. Some level of nonlinearity is present in the results of participants using linear waves due to wave stretching and the drag term of Morison's equation (which uses the square of the wave velocity). Overall, though, we can see that the calculated forces generally agree between participants, with the nonlinearities only creating small changes.

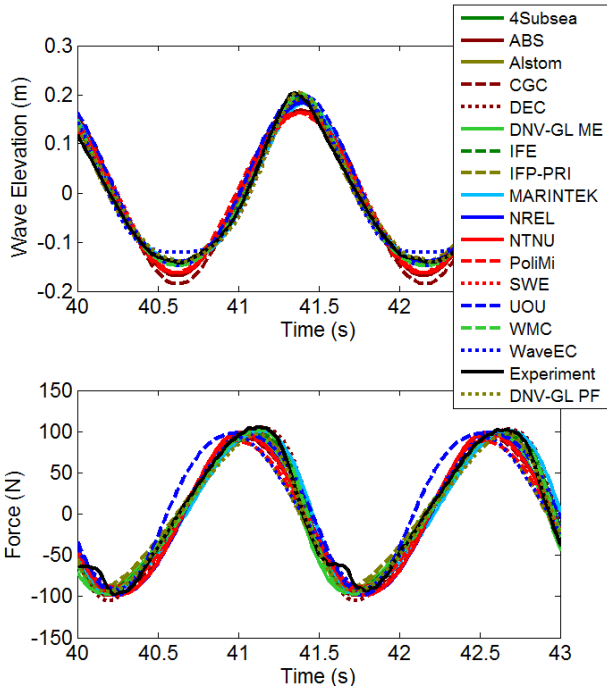


Fig. 6: Wave elevation and force time histories for OC5 Test 4

The nonlinearity of the resulting hydrodynamic force is further evident in Fig. 7, which shows the power spectral density (PSD) of this signal. A prominent peak is present at the wave frequency (0.65 Hz), and one can see a series of harmonics of this frequency at 1.3 and 1.95 Hz. Fig. 8 zooms in on the 2nd peak to show that models using linear wave theory (and some 2nd order theories) are unable to capture the 2nd peak. These lower-order models do capture some of the 3rd peak from the drag force term in Morison’s equation, but the magnitude is not as great as in the measured signal. It was noted previously in this paper that the drag coefficient did not have a significant effect on the total calculated force, but one can see here that having a non-zero value is important for capturing the 3rd peak of the force. This 3rd peak has been shown to be associated with exciting ringing in a structure, and therefore even though it is small, it is important (Stansberg, 1997).

In Fig. 9 and Fig. 10 we look further at the magnitudes of the Fourier peaks shown in Fig. 7. In Fig. 9, the magnitude of the first three peaks of the PSD for each of the 16 regular wave experimental tests are shown normalized by the radius squared multiplied by the amplitude of the wave raised to the power of the order of the peak (1st, 2nd, or 3rd). Through this normalization, the Fourier peak values should theoretically be consistent across all test cases for a given peak order and for a given wave number. This means, for instance, that 1st peak values for Tests 1 through 8 should have roughly the same value. Tests 9 through 16 have a different wave number and will therefore have slightly different values. Deviations from this constant value come from the influence of the size of the cylinder on the flow and the wave steepness. A comparison of the experimental loads with the theoretical FNV solution can be found in (Stansberg, 1997).

The normalized Fourier peak values for the 16 regular wave cases were calculated by all participants. Differences seen in the results were due to the modeling approach and the choice of hydrodynamic parameters. Therefore, to try to focus more on the differences that the modeling approach creates, four of these cases were re-examined with all participants using the same parameters, including wave height, wave period, C_A , and C_D . Bar plots of the resulting first three Fourier peak magnitudes can be seen in Fig. 10.

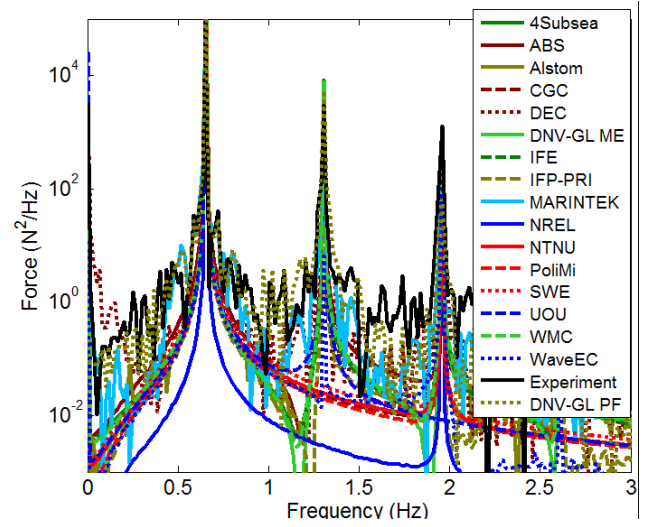


Fig. 7: PSD of total hydrodynamic force for Test 4: light red = linear Airy theory; dark red = linear Airy theory with stretching; blue = 2nd order; other colors = higher order; black = exp. results

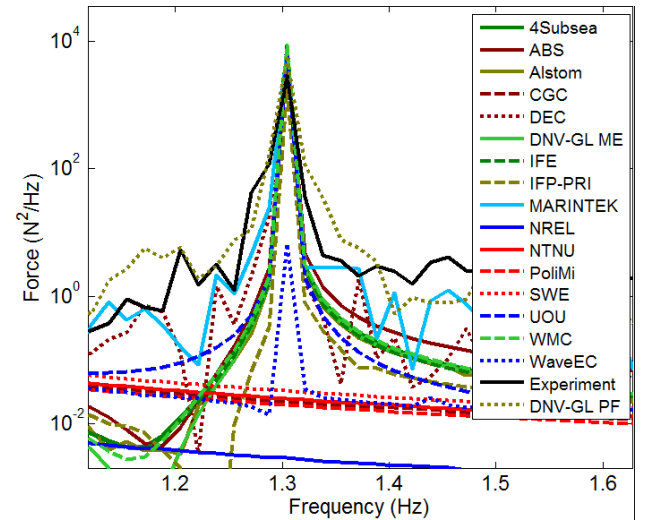


Fig. 8: Zoomed-in view of PSD of Test 4 hydrodynamic force

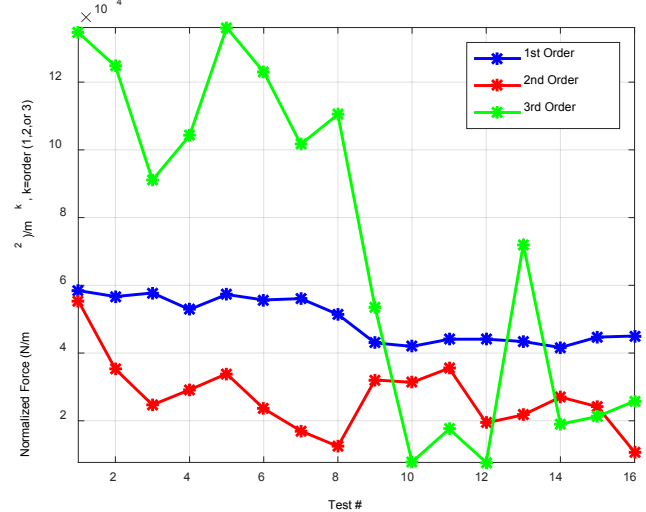


Fig. 9: Experimental forces normalized by radius squared and wave amplitude raised to the power of the peak (1, 2, or 3)

These values are compared to the experimental values. When doing such a comparison, one should keep in mind that there is some level of uncertainty in the reported experimental values. The uncertainty can come from a variety of sources, including: uncertainty in the geometric properties of the system, uncertainties in the installation of the structure and the measurement equipment (such as alignment), calibration of the measurement instruments, and inaccuracies in the measurement equipment (including the data acquisition system). The uncertainty related to the accuracy of the measurement equipment, and the repeatability of the conditions is considered here.

The wave measurements used were not from the actual test in which the force is measured, but rather from a test performed without the structure present. By measuring the wave conditions without the structure present, one is able to obtain the undisturbed wave at the exact location where the model is located. Therefore, we need to understand how repeatable this wave is from the test in which it was measured to the test in which the force was measured. For this experiment, the standard deviation of the wave gauges between multiple experiments was 0.8% for five runs, and the measured force was less than 0.5%. The wave gauges are accurate to 1 mm (a 0.4-0.7% uncertainty), and the force measurement error is estimated at around 2%. These three sources of uncertainty were combined using the square root of the sum of squares of each error, resulting in an overall uncertainty between 2.19% and 2.27%, depending on the height of the wave being considered. These uncertainty levels are shown as bands on the experimental results in Fig. 10.

For the 1st (linear) peak, we see that most of the codes predict the response consistently and are similar to the experimental value. The 1st peak (as shown in Fig. 7) is much larger than the other peaks, which means that the total force calculated by participants is very similar. Differences in the force calculation come in the higher-order components, which can be seen in the 2nd and 3rd Fourier peaks.

For the 2nd peak magnitude (see middle graph in Fig. 10), we see that those using linear theory without stretching do not capture this force, as was shown in the previous power spectral density plots. In addition, NREL and UOU's 2nd order approach cannot capture the force, though MARINTEK can. MARINTEK uses a method for extending the hydrodynamic force above the SWL (consistent with 2nd order theory) that is not applied by NREL or UOU, which means that calculation of the hydrodynamic force up to the instantaneous wave elevation is of greater importance than treatment of the 2nd order potential in the force calculation. Those participants using 1st or 2nd order wave theories and some method to calculate the force up to the instantaneous water level have similar values to those using higher-order theories. In addition, two potential flow solutions from NREL (only Tests 3 and 9) and WavEC incorporate 2nd order potential theory and are also able to capture some of the 2nd harmonic, but with differing results. For Tests 3 and 8, the calculated 2nd peak (harmonic) values are larger than the experimental values. These cases have larger values of $k \cdot R$, where k is the wave number and R is the radius. For larger $k \cdot R$ values, nonslender diffraction effects occur that are not captured by Morison's equation (Stansberg, 1997). These nonslender diffraction effects tend to reduce the experimental value compared to the computed value.

For the 3rd peak forces, the tools with linear wave models (without stretching) now capture some small effect due to the drag force mentioned earlier. Those participants using 1st order wave models that calculate forces up to the IWL do not consistently capture the same level of force as the higher-order models for the 3rd peak, which is contrary to what we saw for the 2nd peak. ABS and CGC, for instance, now have values similar to those using linear wave theory without stretching. This is consistent with Liaw (2000), who states that

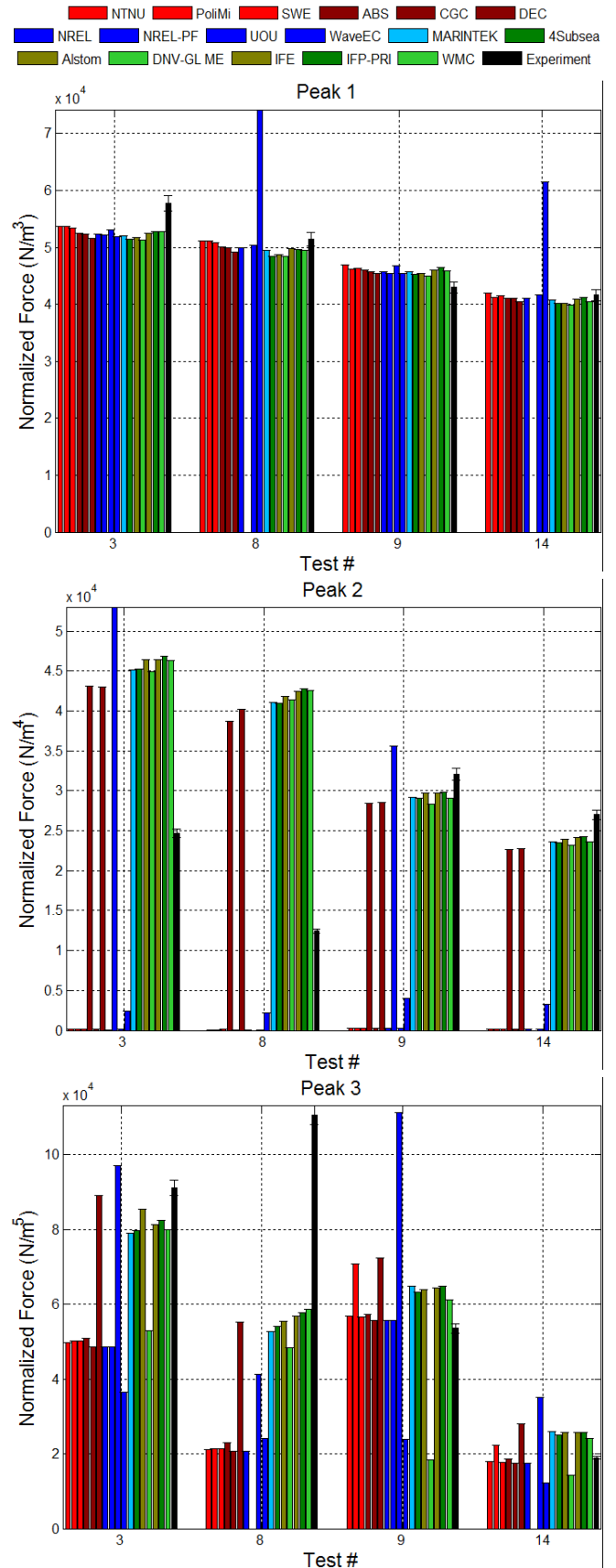


Fig.10: Normalized 1st, 2nd, and 3rd order Fourier amplitudes, using consistent parameters

applying wave stretching to linear wave theory will only produce even-order harmonics, and not 3rd order ones. The majority of codes under-predict the 3rd harmonic force for Tests 3 and 8, in which nonslender diffraction effects are significant, which is the opposite of what we saw for the 2nd peak.

Irregular Wave Tests

Next, the group simulated four different irregular wave tests, which included two different wave conditions and two different cylinder diameters. Tests 17 and 18 had the same wave conditions, as did Tests 19 and 20. The normalized experimental force PSDs (normalized by dividing by R^2) of these four cases can be seen in Fig. 11. Note there is a slight decrease in the PSD magnitude for cases with a larger radius (larger $k*R$). The normalized PSD for Test 17 from participants is shown in Fig 12. The general form of the spectrum is captured by most participants, but it is difficult to identify specific differences because many participants created their own JONSWAP spectrum based on the provided significant wave height and peak period. A plot with only those participants using the direct wave time series as input is shown in Fig. 13. From this plot, one can see that the models are under-predicting the force response throughout the low-frequency range.

Next, one section of the signal is examined in further detail where a particularly steep wave event occurs. This allows us to see how well the models are able to predict events that have a high degree of nonlinearity. These events are important because they may cause high-frequency excitation in the structure, which could result in a ringing response. Only those codes using the exact time series can be investigated because these wave events won't be replicated when only duplicating the wave spectral signature. Fig. 14 shows one such event in Tests 17 and 18 with a high-pass filter applied to focus on the higher-frequency content of the signal. From this figure, one can see that the models predict the peak of the significant wave event around 680.25 s fairly well, but the simulated response immediately after the large wave differs from the experiment, with the experiment exhibiting a higher frequency response than the models. The simulation tools seem to all present similar results, including the potential flow solution by DNV GL.

CONCLUSIONS

This paper presents a summary of the work performed during the first phase of the new OC5 project operating under Task 30 of IEA Wind. This project represents the first step towards validating the capability of offshore wind modeling tools to accurately model physical systems. This first project examined a fairly simple structure to better focus on (and understand) the differences in how the tools model hydrodynamic loads.

The first step of the work was to calibrate the model and wave parameters. For the model, this included calibration of the hydrodynamic coefficients. For the waves, this included calibration of the wave height and period. The calibration was done independently by the participants, using the method of their choice. The calibrated values for wave height and period were fairly consistent among the project participants; much larger variation was observed in the calibration of the hydrodynamic coefficients. The drag coefficient had the most variation, probably due to its insensitivity to the inertia-dominated forces. Participants found that the best approaches for choosing the coefficients was to either use look-up tables (such as from DNV) or to use a weighted least-squares approach on a subset of the data. The decision at the end of the calibration process was to move forward with validation work, allowing participants to use their own calibrated values for the model and wave parameters. The only exception was for

the wave periods, which had small differences among participant's calibrated values, and were thus set to prescribed values for ease in comparing the computed forces.

Four of the 20 test cases were used for the calibration, and the remaining 16 for validation. The validation cases included 12 regular wave cases and 4 irregular ones. For the validation cases, the participants were given the experimental wave time history and were asked to report the resulting integrated hydrodynamic force in the x -direction. The most important finding from examination of the force results was the varying levels of nonlinear behavior in the models. As the waves became larger, they also became more nonlinear, and those using higher-order wave theories were able to better approximate the shape of the wave elevation and resulting hydrodynamic forces. Most of the codes were able to capture the 1st order forces fairly well, but only higher-order wave models could capture the 2nd and 3rd order harmonic force components. For larger $k*R$ values, nonslender diffraction effects reduce the 2nd harmonic forces in the experimental data, as compared to the simulated data. The 3rd harmonic forces are key in the prediction of ringing loads, and most participants under-predict this component, especially for higher $k*R$ values. In addition, it was found that calculating loads up to the instantaneous wave elevation, either through a high-order wave model or through a wave stretching technique, is important in capturing the 2nd harmonic force, more so than treating higher-order potentials. While inconsistent results were seen, it appears that one needs at least 2nd order wave loads and calculation of the force up to the IWL to capture most of the 3rd harmonic force. This requirement would mean that linear theory with stretching will not be able to capture ringing loads.

This work has shown the importance of higher-order theory in accurately predicting the hydrodynamic loading on a structure. Further analysis of hydrodynamic loads on cylinders will be performed within OC5 using a data set obtained from testing that was performed by DHI and DTU. We hope to include CFD simulations in the analysis of this next data set to further illuminate the deficiencies of the engineering hydrodynamic force models, and identify appropriate methods for making them more accurate. Phase II of the project will then focus on the validation of a floating offshore wind system, also tested in a tank environment.

ACKNOWLEDGEMENTS

A number of academic and industrial project partners from 11 different countries participated in the task. Those actively involved in Phase I are: the National Renewable Energy Laboratory (NREL - USA), MARINTEK (Norway), 4Subsea (Norway), Norwegian University of Science and Technology (NTNU - Norway), Politecnico di Milano (PoliMi - Italy), Stuttgart Wind Energy (SWE - Germany), the Institute for Energy Technology (IFE - Norway), DNV GL (UK), ABS (USA), Alstom (Spain), Chinese General Certification (CGC - China), DongFang Electric Corporation (DEC - China), Goldwind (China), IFPEN/PRINCIPIA (France), University of Tokyo (Japan), University of Ulsan (UOU - Korea), Wave Energy Center (WavEC - Portugal), and Knowledge Centre WMC (the Netherlands).

We would like to acknowledge Carl Trygve Stansberg at MARINTEK for graciously supplying the data and information needed for this first phase of the OC5 project. This work was supported by the U.S. Department of Energy under Contract No. DE-AC36-08GO28308 with the National Renewable Energy Laboratory. Funding for the work was provided by the DOE Office of Energy Efficiency and Renewable Energy, Wind and Water Power Technologies Office.

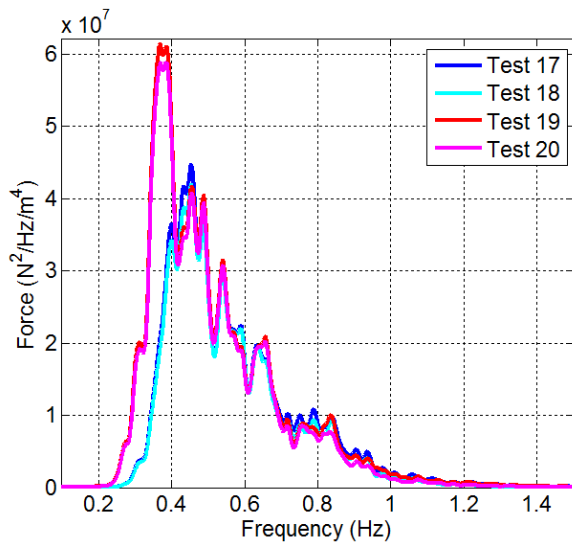


Fig. 11: Normalized force PSDs of the four irregular wave tests

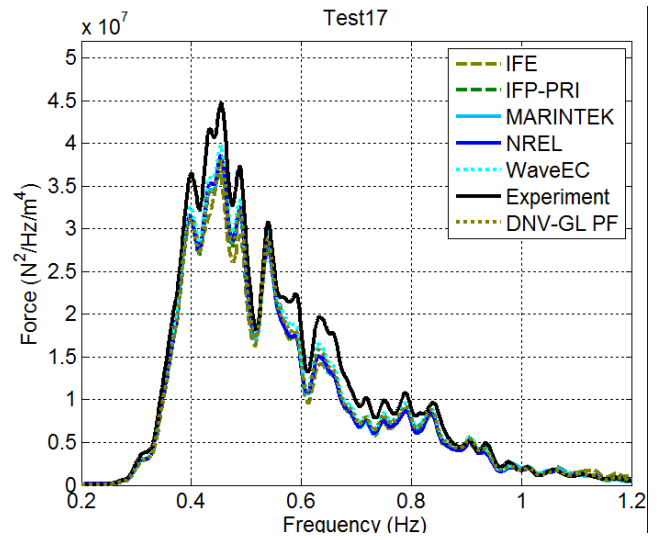


Fig. 13: Normalized force PSDs for irregular wave tests from participants using direct input of the wave time history (Test 17)

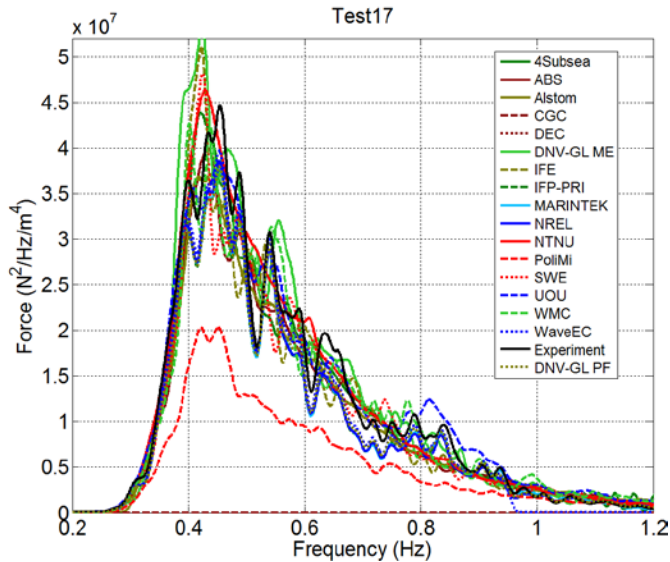


Fig.12: Normalized force PSDs for irregular wave test 17 from all participants

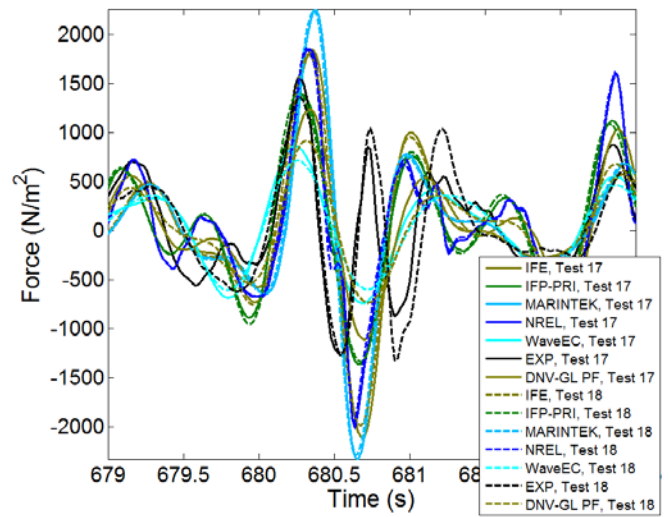


Fig.14: Normalized force for steep wave event in Test 17 and Test 18

REFERENCES

DNV, Recommended Practice DNV-RP-C205 (2010). "Environmental Conditions and Environmental Loads."

Gudmestad, Ove T.; Moe, Geir (1996). "Hydrodynamic coefficients for calculation of hydrodynamic loads on offshore truss structures", *Marine Structures*, 9, 745–758.

Liaw, C. Y. (2000), "Inundation Effect of Wave Force on Jack-Up Platforms", *Proceedings of the 10th International Offshore and Polar Engineering Conference*.

Marthinsen, T.; Stansberg, C.T.; and Krokstad, J.R., (1996). "On the Ringing Excitation of Circular Cylinders", *Proceedings of the Sixth International Offshore and Polar Engineering Conference*.

Morison, J. R.; O'Brien, M. P.; Johnson, J. W.; Schaaf, S. A. (1950). "The force exerted by surface waves on piles", *Petroleum Transactions (American Inst. of Mining Engineers)* 189, 149–154.

Robertson, A.; et al. (2014). "Offshore Code Comparison Collaboration, Continuation within IEA Wind Task 30: Phase II Results Regarding a Floating Semisubmersible Wind System". *The Ocean, Offshore and Arctic Engineering Conference*. NREL Report No. CP-5000-61154.

Sarpkaya, T.; Isaacson, M. (1981). "Mechanics of wave forces on offshore structures", New York: Van Nostrand Reinhold, ISBN 0-442-25402-4.

Stansberg, C.T.; Krokstad, J.R.; and Lehn, E. (1995). "Experimental Study on Non-Linear Loads on Vertical Cylinders in Steep Random Waves," *Proceedings of the Fifth International Offshore and Polar Engineering Conference*.

Stansberg, C.T. (1997). "Comparing Ringing Loads from Experiments with Cylinders of Different Diameters – An Empirical Study", *Proceedings, vol. 2, the BOSS '97 Conference, Delft, The Netherlands*.